Comparison of Solvent Extraction and Extraction Chromatography Resin Techniques for Uranium Isotopic Characterization in High-Level Radioactive Waste and Barrier Materials

Santiago Hurtado-Bermúdez[1], María Villa-Alfageme[2], José Luis Mas[3], María Dolores Alba[4]

[1]*Centro de Investigación Tecnología e Innovación, Universidad de Sevilla (CITIUS). Av. Reina Mercedes 4B. 41012 Sevilla, Spain*

[2]*Dpto. Física Aplicada II, ETSIE. Av. Reina Mercedes 4A. Universidad de Sevilla. 41012-Sevilla, Spain*

[3]*Dpto. Física Aplicada I, Escuela Universitaria Politécnica. Universidad de Sevilla, Spain*

[4]*Instituto Ciencia de los Materiales de Sevilla, CSIC-Universidad de Sevilla, Avda, Américo Vespucio, 49, Sevilla, Spain*

Abstract

The development of Deep Geological Repositories (DGP) to the storage of high-level radioactive waste (HLRW) is mainly focused in systems of multiple barriers based on the use of clays, and particularly bentonites, as natural and engineered barriers in nuclear waste isolation due to their remarkable properties.

Due to the fact that uranium is the major component of HLRW, it is required to go in depth in the analysis of the chemistry of the reaction of this element within bentonites. The

determination of uranium under the conditions of HLRW, including the analysis of silicate matrices before and after the uranium-bentonite reaction, was investigated. The performances of a state-of-the-art and widespread radiochemical method based on chromatographic UTEVA resins, and a well-known and traditional method based on solvent extraction with tri-n-butyl phosphate (TBP), for the analysis of uranium and thorium isotopes in solid matrices with high concentrations of uranium were analysed in detail.

In the development of this comparison, both radiochemical approaches have an overall excellent performance in order to analyse uranium concentration in HLRW samples. However, due to the high uranium concentration in the samples, the chromatographic resin is not able to avoid completely the uranium contamination in the thorium fraction.

Keywords

high-level radioactive waste; UTEVA; TBP; uranium; thorium

1. Introduction

Many researchers are devoted to the development of Deep Geological Repositories (DGP) to the storage of high-level radioactive waste (HLRW). Mainly the selected solution is based on a system of multiple barriers. Most of security of the disposal relies on an engineered barrier. Clays are ideal materials for natural and engineered barriers for nuclear waste isolation due to their high sorption capacity, low permeability, and swelling capability. In experimental conditions, it is found that the radioactive wastes are immobilised and their diffusion prevented trough physical-chemical mechanism with a clay barrier, such as precipitation, adsorption or a chemical reaction including the formation of secondary stable mineral phases. At present, bentonite is established as the most appropriate clay to form the engineered barrier in the DGP (Kaufhold et al., 2015).

Previous papers have analysed the capacity of retention and the kinetics reaction properties of bentonites in relation to several radionuclides such us ^{152}Eu (Alba et al., 2011; Mrabet

et al., 2014; Villa-Alfageme et al., 2014), additionally trivalent simulators of actinides have been used to study their potential retention capacity of HLRW by bentonites (Alba et al., 2009; Alba and Chaín, 2007). Determination of radionuclides in HLRW is important for nuclear waste management. Because uranium is the major component of HLRW, it is required to go in depth in the analysis of the chemistry of this element within bentonites and other clays and for this, specific radiochemical methods must be developed. Additionally, uranium undergoes a decay chain containing several radioactive isotopes, such as thorium and polonium, that have also to be analysed within HLRW.

A complete control of the geochemical behaviour of uranium under the specific conditions created by HLRW includes the analysis of silicate matrices before and after the uranium-bentonite reaction. Because this step is crucial when performing a complete study of the reaction properties of the system uranium-bentonite. It is then key to develop suitable methods for this kind of determinations.

Among the methods proposed in the literature to determine uranium in several matrices, the most recent ones are focused on behaviour of selected fission products and actinides on UTEVA resin (Skinner and Knight, 2016), purification of uranium using *n*-tri butyl phosphate (TBP) as extractant and *n*-decanol as phase modifier (Pradeep and Biswas, 2017), extraction of uranium from simulated highly active feed in a micromixer-settler with 30% TBP and 36% TiAP solvents (Kumar et al., 2017), diluted salts by TBP and dialkyl amides (Ansari et al., 2016), or uranyl selective polymeric membrane electrodes (Badr et al., 2014). However, it is not analysed the suitability and the sensitivity of currently available radiochemical methods when uranium must be quantified in complex matrices related to HLRW.

For this reason, in this study the performances of one state-of-the-art and widespread radiochemical method for the analysis of uranium (and additionally thorium and polonium) isotopes in solid matrices (Mas et al., 2012) was analysed in detail when it is applied to the measurement of matrices with high concentrations of uranium. This method combines a sequential separation of polonium-thorium-uranium using chromatographic UTEVA (Triskem Int.) resins and alpha spectrometry as radiometric measurement method.

Additionally, a well-known and traditional method was used to compare the performance of the UTEVA resins. In that case, uranium and thorium were extracted using tri-n-butyl phosphate (TBP) as solvent extraction method, combined with AG1-X8 ion-exchange resin (Villa et al., 2011). This method has the main drawback that is time consuming, but is a routine and robust method to extract uranium, thorium and plutonium as part of the nuclear reprocessing process (Dey and Bansal, 2006).

The analysed matrices were uranyl nitrates, and bentonites after a hydrothermal treatment with uranyl nitrate. The main objective of this paper is to analyse the performance of the UTEVA method to be used as a routine method to evaluate uranium, and additionally thorium and polonium, in HLRW samples, where high uranium concentrations are expected.

2. Experimental

2.1. Sample preparation

In the comparative study between both radiochemical methods, a simulated HLW material was prepared by using two different matrices: uranyl nitrate 6-hydrate $UO_2(NO_3)_2 \cdot 6H_2O$ (supplied by Panreac) and FEBEX bentonite (from the Cortijo de Archidona deposit, Almería, Spain) (Enresa, 2000). Eight aliquots of this simulated HLW material were prepared and arranged in two groups.

In a first group, four aliquots of 0.0048 g of pure uranyl (0.0022 g of uranium) were analysed. ^{232}U, ^{229}Th and ^{209}Po were initially added to the aliquots as internal tracers. The first two aliquots (U-UTEVA-1 and U-UTEVA-2) were analysed following the UTEVA procedure later described, and only the second two aliquots (U-TBP-1 and U-TBP-2) were analysed following the TBP extraction procedure because it is a well-established method that we use as standard method of analysis.

In a second group, a total of four aliquots were prepared to check the performance of UTEVA chromatographic resin. ^{232}U was added as internal tracer to those four aliquots in order to quantify uranium separation through UTEVA columns and subsequent alpha

106 spectrometry measurement. First, two aliquots of uranyl nitrate were prepared containing
107 0.55 g of pure uranyl (corresponding to 0.260 g of uranium), and labelled as URANYL-1
108 and URANYL-2. These results were checked against the previous results from the first
109 group of aliquots.

110 Second, two aliquots were prepared by the hydrothermal reaction of 0.032 g of uranyl
111 (0.015 g of uranium) with 300 g FEBEX bentonite and 1.1 g of $ZrO(NO_3)_2 \cdot 7H_2O$ (as
112 tetravalent simulator of uranium) (Villa-Alfageme et al., 2014). After the hydrothermal
113 reaction, the solid and liquid remnant were examined. The solid product aliquot contained
114 reacted bentonite, zircon silicate and reacted uranium in both phases (labelled as ZrU-
115 Solid) (Villa-Alfageme et al., 2015). The liquid product aliquot contained dissolved zircon
116 and uranium (labelled as ZrU-Liquid). Additionally, in order to validate the analysis of the
117 two aliquots (ZrU-Solid and ZrU-Liquid), a comparison with gamma-ray spectrometry
118 technique was carried on.

119 ### *2.2. UTEVA chromatographic extraction method*

120 This procedure was adapted from (Mas et al., 2012) for the matrices described and it is
121 schematized in Fig. 1a.

122

123 1. *Digestion of the solid matrix*. Uranyl samples were digested with concentrated
124 nitric acid. Whereas bentonites were total digested by a combination of HNO_3-
125 HCl-HF (5 mL - 2 mL - 1 mL). Samples were gently heated and stirred until
126 complete dissolution and taken to dryness. Residue is again dissolved in 15 mL
127 of 8 mol L^{-1} nitric acid.

128 2. Fe^{3+} carrier was added and pH raised to 8.5 with ammonium hydroxide to get
129 the precipitation of iron hydroxides and actinides, the supernatant was removed
130 by siphoning and discarded after settling for at least 8 h.

3. UTEVA column was preconditioned loading 3.5 mL of 3 mol L^{-1} HNO_3 three times.

4. Precipitate was dissolved in 15 mL of 3 mol L^{-1} HNO_3 - 1 mol L^{-1} $Al(NO_3)_3$ and 200 mg ascorbic acid. Dissolved sample was loaded into the resin.

5. *Elution of Am/Pu/Sr/Po/Ra*. The column was rinsed with 5 mL of 3 mol L^{-1} HNO_3 - 1 mol L^{-1} $Al(NO_3)_3$, afterwards with 10 mL of 3 mol L^{-1} HNO_3 three times and finally rinsed with 5 mL of 9 mol L^{-1} HCl (Oliveira and Carvalho, 2006).

6. *Elution of thorium*. Column was rinsed with 4 mL of 5 mol L^{-1} HCl - 0.05 mol L^{-1} oxalic acid five times eluting the thorium fraction.

7. *Elution of uranium.* The column was finally rinsed with 5 mL of 1 mol L^{-1} HCl three times eluting the uranium fraction.

2.3. TBP liquid-liquid solvent extraction method

The procedure followed for the uranium, thorium and polonium separation was adapted from the TBP procedure described in (Martínez-Aguirre, A., García-León, M., Ivanovich, 1994). It is outlined in Fig. 1b and is in detail below:

1. Pretreatment of the sample was carried out following step 1 described in *2.2*.

2. Uranium was precipitated with iron hydroxide and then taken to dryness on a hot plate.

3. The precipitate was dissolved in 10 mL of 8 mol L^{-1} HNO_3 and introduced into a 50 mL funnel for the solvent extraction.

4. 5 mL TBP were added to the funnel.

5. *Extraction of polonium*. The funnel was shaken for 15 min and the aqueous phase removed. Additionally, 10 mL of 8 mol L^{-1} HNO_3 were added and the process repeated. This was repeated three times to get an aqueous final solution of 30 mL containing the polonium.

6. 20 mL Xilene were added to the funnel.

7. *Extraction* of *thorium*. 15 mL of 1.5 mol L^{-1} HCl were added to the funnel and the solution shaken for 10 minutes. The aqueous phase was removed and the process was repeated three times to finally obtain 45 mL of HCl solution, containing thorium (including eventually some traces of uranium).

8. Extraction *of uranium*. 15 mL of MiliQ water were added and the solution was shaken for 10 minutes. The aqueous phase was removed and the process was repeated again three times to get 45 mL of H_2O solution, containing the uranium fraction.

9. Purification *of thorium*. Thorium solution obtained from the solvent extraction might present traces of uranium, for this reason it was essential to make a final purification of thorium. This was done by chromatographic separation in a glass column (height h = 10 cm; diameter 1 cm). 6.5 mL of AG1-X8 resin was added to the column and preconditioned with 10 mL 9 mol L^{-1} of HCl twice. Thorium solution was taken to dryness, redissolved in 4 x 10 mL of 9 mol L^{-1} HCl and loaded into the column. Resin was rinsed three times with 10 mL of 9 mol L^{-1} HCl. Uranium was retained by resin and a purified Th fraction was recovered in the eluted solution.

2.4. Alpha-particle spectrometry

Purified uranium and thorium phases were electroplated onto stainless steel discs (Martínez-Aguirre, A., García-León, M., Ivanovich, 1994) and measured and polonium was self-deposited onto a silver disk (Le Moigne et al., 2013). Counting of thorium, uranium (electro-deposited) and polonium (self-deposited) isotopes was done using alpha

detector PIPS type (Canberra) in an array comprised of 10 chambers. Measurements were undertaken at CITIUS (Centro de Investigación, Tecnología e Innovación, Universidad de Sevilla) laboratory at Universidad de Sevilla. The resolution of the peaks was found to be between 60 and 40 keV in all cases.

2.5. Gamma-ray spectrometry

The gamma-ray measurements were carried on by a Canberra n-type hyper-pure germanium gamma-ray detector (HPGe), located at Centro de Investigación, Tecnología e Innovación Universidad de Sevilla, CITIUS, with a nominal relative photo-peak efficiency of 60% at 1332 keV. The detector chamber was set up by a lead shield (10 cm thick standard lead) and an inner copper layer (5 mm) protecting the detector against environmental background radiation. The electronic chain consisted of a Canberra preamplifier 2002, and a Canberra Inspector 2000 DSP digital electronic chain. Gamma-ray spectra were analysed with Genie2K software.

Hydrothermal reaction products were collected by filtration using 0.45 μm Milipore filters and air-dried at 60 ºC. In order to measure natural ^{235}U activity in the sample, the gamma-ray emission of 143.8 keV (10.9% total yield) was selected.

Counting efficiencies were calculated through Monte Carlo simulations using LABSOCS program (Hurtado and Villa, 2010) for the two counting geometries used: a 0.45 μm Millipore filter (ZrU-Solid) and a 100 mL cylindrical beaker (ZrU-Liquid). The composition of the solid sample was essential to compute correctly the simulated efficiency of this counting geometry.

Finally, Monte Carlo efficiencies were successful compared to the experimental ones obtained through the preparation of solid and aqueous standards spiked with a known amount of diluted uranyl solution.

2.6. Scanning electron microscopy

The morphology and chemical composition of the hydrothermal products were investigated using a SEM-FEG HITACHI S-4800 a scanning electron microscope equipped with an

Xflash 4010 (BRUKER) for energy dispersive X-ray (EDX) analysis, located at Microscopy Service in ICMS (CSIC-Universidad de Sevilla).

3. Results and discussion

In this section, the obtained activities and isotopic ratios using both radiochemical methods are shown for each isotope fraction, and a discussion about the chemical recovery, cross-contamination, and maximum load capacity is carried out.

3.1. Uranium fractions

The results obtained for uranium activity for each aliquot and radiochemical method (TBP or UTEVA) are presented in Table 1 and Fig. 2. The components contributing to the combined measurement uncertainty such as count rates of sample and tracer, chemical recovery, tracer activity and mass of the sample and the tracer are calculated as one standard deviation.

Table 1 shows that both UTEVA column method and TBP method are capable of extracting the uranium from the analysed aliquot with an acceptable chemical yield. The chemical yield using the added ^{232}U internal tracer is around 45% for the solvent extraction method and 65% for the chromatographic extraction method.

With respect to the isotopic ratios, the values obtained for ^{234}U and ^{238}U ($^{234}U/^{238}U$), and ^{235}U and ^{238}U ($^{235}U/^{238}U$) are 0.45 and 0.095 respectively. These values do not correspond to those of natural uranium, ~1 and 0.046 respectively (Brennecka et al., 2010). However, this is in agreement with the values measure in commercial uranium reagents (Iturbe, 1992). Specifically, the $^{234}U/^{238}U$ isotopic ratio for U-UTEVA-2 sample is 20% lower than the ratios obtained for U-TBP-1, U-TBP-2 and U-UTEVA-1 samples, and it is also 40% higher for the $^{235}U/^{238}U$ ratio (see Table 1). It can be asserted that this behaviour is not due to the pre-treatment because this step is common for samples U-TBP-1, U-TBP-2, U-UTEVA-1 and UTEVA-2. This effect has not been observed in the analysis of environmental samples following UTEVA method. Further studies should be conducted in that respect.

On the other hand, thorium was not detected in any of the two methods in the electrodeposited U fraction. Since thorium concentration is very small in uranyl matrices, thorium contamination in U fraction was evaluated from the analysis of ^{229}Th tracer.

One of the drawbacks of the use of UTEVA resins for uranium analysis is its limitation on the maximum accepted uranium concentration and its dependence on the type of matrix. The manufacturer recommends a maximum load capacity of the UTEVA resin (Triskem Int.) for U is approximately 0.015 g per 2 mL of the pre-packaged UTEVA columns. In order to check the UTEVA performance several experiments were carried out using only UTEVA columns for the analysis of two aliquots of pure uranyl (URANYL-1, URANYL-2). In the experiments with pure uranyl the maximum capacity of the column for the measurement of U was exceeded, since 0.260 g of uranyl was analysed. The results in Table 2 show that the chemical yields drop below 1% when exceeding the capacity of the column. These results indicate that for UTEVA method it is very important not exceed the load capacity, because the chemical yield decreases drastically, and therefore, an increase of the resin weight required to analyse samples with high concentration of uranium is cost-prohibitive.

Additionally, as in most analytical situations, the presence of significant concentrations of matrix elements can affect the proper operation of methods based on UTEVA resin (Horwitz et al., 1992). Therefore, the performance of these resins was evaluated also in matrices with high silicate content (high refractory fraction). In order to check the UTEVA performance several experiments were carried out using only UTEVA columns for the analysis of two aliquots of zirconium-uranium disilicate, formed after a hydrothermal treatment with FEBEX and $ZrO(NO_3)_2$-$UO_2(NH_3)_2$ (Villa-Alfageme et al., 2015), containing the solid fraction (ZrU-Solid) and the liquid one (ZrU-Liquid) (see Section 2.1. for description).

The characterization of the solid fraction was carried out through SEM micrographs of the reacted FEBEX with ZrO^{2+} (Fig. 3). The solid sample shows lamellar particles with a chemical composition consisting mainly of ZrO^{2+} as interlayer cations (Figs. 3a–3d), and agglomerations of small particles with brilliant appearance (Fig. 3b, point 1) with a

chemical composition compatible with phase containing zirconium (Fig. 3e). Moreover, the SEM/EDX analysis of a different zone (Fig. 3c, point 2) indicated that the treated clay mineral contain iron, probably released upon degradation of the container (Fig. 3f).

Finally, the ZrU-Solid and ZrU-Liquid samples were analysed using both UTEVA radiochemical method and alpha-particle spectrometry, and gamma-ray spectrometry technique. This all translates in the results shown in Table 2. The activity of ^{235}U for ZrU-Solid and ZrU-Liquid samples through gamma-ray spectrometry was 7.6±1.5 Bq and 3.5±1.4 Bq respectively. Both methods give results in total agreement validating the use of UTEVA resin for the analysis of complex matrices.

3.2. Thorium fractions

The results obtained for the concentrations of thorium activity for each aliquot and radiochemical method are presented in Table 3.

Natural thorium is not measured in the Th fraction above the limit of detection through any of the radiochemical methods. The chemical yields obtained through ^{229}Th are similar to those obtained for the U fraction. According to the obtained thorium yields, both methods are apparently suitable for Th measurements.

However, the percentage of U in the Th fraction of the analysed samples has been obtained and shown in Fig. 4. Note that a significant difference between the two methods (UTEVA and TBP) is shown in relation to the Th detected. In the samples separated by UTEVA chromatography columns (U-UTEVA-1 and U-UTEVA-2), U isotopes peaks clearly appear in the Th fraction contaminating the results. The contamination of U has been possibly detected because the analysed samples were with higher activities than natural samples (clay, rock) (about 10 Bq). This contamination of U in the Th fraction is not usually observed in the analysis of low-level environmental samples by UTEVA method because the percentage of the initial U activity presented in the spectra of Th was calculated to be a 1.5% approximately. On the other hand, this contamination does not exist in the samples separated by the TBP solvent extraction method.

Therefore, the U-Th separation procedure using UTEVA columns efficiently separates the Th fraction from uranium, but about 1.5% of the initial uranium contaminates the Th fraction (Mas et al., 2012). This is especially relevant in those matrices where the activity of U is at least one order of magnitude higher than the activity of Th. This contamination may be drastically reduced using a second chromatographic column in tandem, but this can mean substantially higher cost. A TEVA column could be attached to the top end of the UTEVA column, absorbing TEVA resin strongly thorium (IV) from nitric acid solution, and extracting UTEVA resin all tetravalent actinides, including U, from the same nitric acid solution.

3.3. Polonium fraction

The results obtained for the concentrations of polonium activity for each aliquot and radiochemical method are presented in Table 4. Radiochemical yields around 55-60% are obtained for both methods using ^{209}Po as tracer.

It must be highlighted the need to place the silver disk vertically during the autodeposition process, and finally washing it with acetone and distilled water to avoid the deposition of U traces on the disk. This is important in this case due to the very high concentration of uranium in the sample.

Finally, traces of natural ^{210}Po in uranyl samples were detected. The origin is the decay chain of ^{238}U. However, high uncertainties for the activities are obtained because these activities are very close to the minimum detectable activity.

4. Conclusions

The standard TBP method has proven to be an efficient and robust technique to analyse uranium and thorium concentration for all kinds of samples (either HLRW or low-level environmental samples). On the other hand, the uranium-thorium separation method using UTEVA columns works efficiently even applied in complex matrices. However, UTEVA radiochemical method reaches a total separation of the uranium fraction from thorium fraction, but a maximum of 1.5% of the initial uranium contaminates the Th fraction. This

is especially relevant in those matrices where the concentration of U is orders of magnitude higher than that of Th. Therefore, further studies should be carried out to elucidate the use of UTEVA resins in the analysis of HLRW materials.

Acknowledgements

We would like to thank to ENRESA (contract nº 0079000237) and to the Spanish State Program R+D +I oriented societal challenges and FEDER (Project MAT2015-63929-R) for financial support.

338 Tables

339

340 **Table 1.** Activity (Bq) and isotopic ratios of the uranium isotopes using the radiochemical
341 method with TBP (U-TBP-1 and U-TBP-2) and the radiochemical method with UTEVA
342 (U-UTEVA-1 and U-UTEVA-2). MDA is the Minimum Detectable Activity.

Sample	**^{234}U (Bq)**	**± σ**	**^{235}U (Bq)**	**± σ**	**^{238}U (Bq)**	**± σ**
U-TBP-1	10.8	0.3	2.19	0.07	23.6	0.7
U-TBP-2	10.7	0.3	2.18	0.07	23.4	0.7
U-UTEVA-1	9.9	0.3	2.18	0.07	22.1	0.7
U-UTEVA-2	9.0	0.3	3.25	0.10	23.9	0.7
Sample	**^{234}U/^{238}U**	**^{235}U/^{238}U**	**^{232}U recovery**	**MDA ^{234}U (Bq)**	**MDA ^{235}U (Bq)**	**MDA ^{238}U/ (Bq)**
U-TBP-1	0.46	0.093	44%	0.05	0.08	0.06
U-TBP-2	0.46	0.093	47%	0.05	0.07	0.06
U-UTEVA-1	0.45	0.099	63%	0.04	0.08	0.05
U-UTEVA-2	0.38	0.136	65%	0.05	0.09	0.05

343

344

345

346

347

348

349

350

351

352

353

354

355 **Table 2.** Activity (Bq) and isotopic ratios (in activity) of the uranium isotopes using the
356 UTEVA radiochemical method for pure uranyl matrices (URANYL-1 and URANYL-2)
357 and the product of a hydrothermal treatment with FEBEX and $ZrO(NO_3)_2$-$UO_2(NH_3)_2$ in
358 the solid fraction (ZrU-Solid) and liquid (ZrU-Liquid). Chemical yields are not included
359 for samples under hydrothermal treatment, since most of the uranium is lost in that process,
360 not during the radiochemical procedure. MDA is the Minimum Detectable Activity.

361

Sample	**^{234}U (Bq)**	**± σ**	**^{235}U (Bq)**	**± σ**	**^{238}U (Bq)**	**± σ**
URANYL-1	666	79	144	17	1541	183
URANYL-2	548	92	78	13	1120	189
ZrU-Solid	52.9	2.4	7.9	0.4	109.3	5.0
ZrU-Liquid	16.1	4.6	3.0	0.7	36.2	7.1
Sample	**^{234}U/^{238}U**	**^{235}U/^{238}U**	**^{232}U recovery**	**MDA ^{234}U (Bq)**	**MDA ^{235}U (Bq)**	**MDA ^{238}U/ (Bq)**
URANYL-1	0.432	0.0938	0.54%	0.05	0.08	0.06
URANYL-2	0.489	0.0695	0.30%	0.05	0.07	0.06
ZrU-Solid	0.485	0.0723	--	0.04	0.08	0.05
ZrU-Liquid	0.446	0.0830	--	0.05	0.09	0.05

362

363

364

365

366

367

368

Table 3. Activity (Bq) of thorium isotopes using the radiochemical procedure with TBP (U-TBP-1 and U-TBP-2) and the radiochemical process with UTEVA (U-UTEVA-1 and U-UTEVA-2). The chemical recovery is shown through ^{229}Th. MDA is the Minimum Detectable Activity.

Sample	**^{230}Th(Bq)**	**± σ**	**^{232}Th (Bq)**	**± σ**	**^{229}Th recovery**	**MDA ^{230}Th (Bq)**	**MDA ^{232}Th (Bq)**
U-TBP-1	< MDA		< MDA		60	0.12	0.06
U-TBP-2	< MDA		< MDA		52	0.04	0.05
U-UTEVA-1	< MDA		< MDA		71	0.07	0.03
U-UTEVA-2	< MDA		< MDA		51	0.05	0.05

Table 4. Activity (Bq) of ^{210}Po using the radiochemical procedure with TBP (U-TBP-1 and U-TBP-2) and the chemical procedure with UTEVA (U-UTEVA-1 and U-UTEVA-2). MDA is the Minimum Detectable Activity.

Sample	^{210}Po (Bq)	± σ	MDA (Bq)
U-TBP-1	0.00025	0.00013	0.00024
U-TBP-2	0.00064	0.00017	0.00021
U-UTEVA-1	0.00069	0.00017	0.00016
U-UTEVA-2	0.00045	0.00011	0.00016

Table captions

Table 1. Activity (Bq) and isotopic ratios of the uranium isotopes using the radiochemical method with TBP (U-TBP-1 and U-TBP-2) and the radiochemical method with UTEVA (U-UTEVA-1 and U-UTEVA-2). MDA is the Minimum Detectable Activity.

Table 2. Activity (Bq) and isotopic ratios (in activity) of the uranium isotopes using the UTEVA radiochemical method for pure uranyl matrices (URANYL-1 and URANYL-2) and the product of a hydrothermal treatment with FEBEX and $ZrO(NO_3)_2$-$UO_2(NH_3)_2$ in the solid fraction (ZrU-Solid) and liquid (ZrU-Liquid). Chemical yields are not included for samples under hydrothermal treatment, since most of the uranium is lost in that process, not during the radiochemical procedure. MDA is the Minimum Detectable Activity.

Table 3. Activity (Bq) of thorium isotopes using the radiochemical procedure with TBP (U-TBP-1 and U-TBP-2) and the radiochemical process with UTEVA (U-UTEVA-1 and U-UTEVA-2). The chemical recovery is shown through ^{229}Th. MDA is the Minimum Detectable Activity.

Table 4. Activity (Bq) of ^{210}Po using the radiochemical procedure with TBP (U-TBP-1 and U-TBP-2) and the chemical procedure with UTEVA (U-UTEVA-1 and U-UTEVA-2). MDA is the Minimum Detectable Activity.

Figures

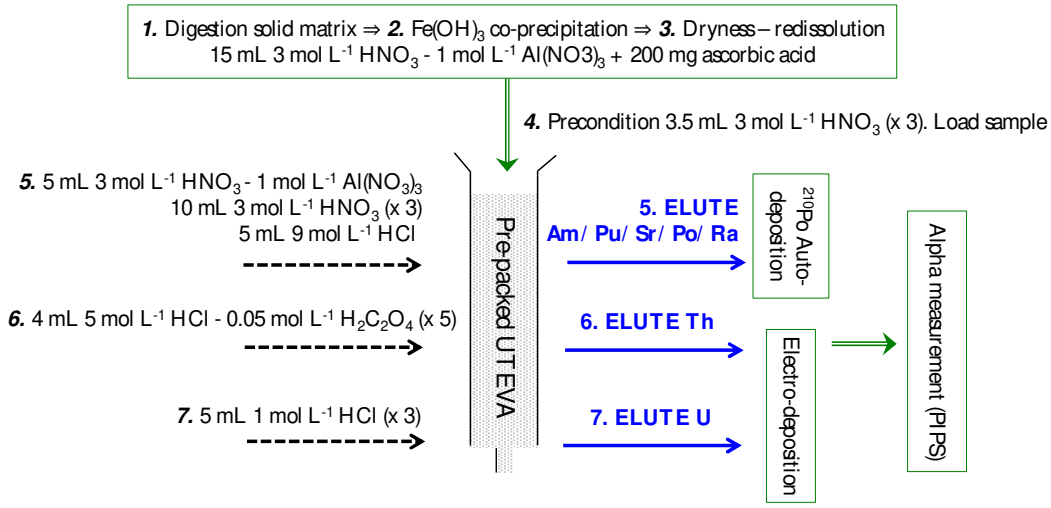

425

426 **Fig. 1a.** UTEVA chromatographic extraction method.

427

428

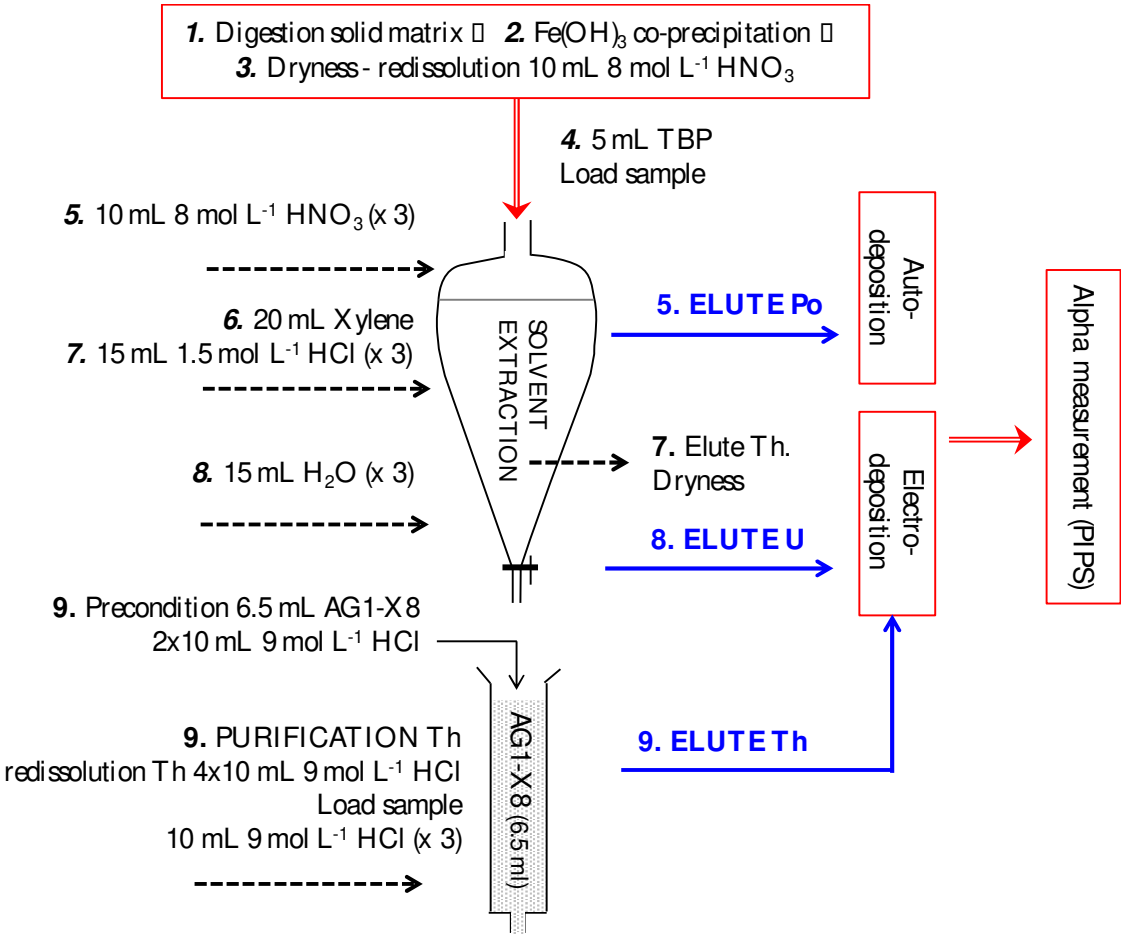

429

430 **Fig. 1b.** TBP liquid-liquid solvent extraction method.

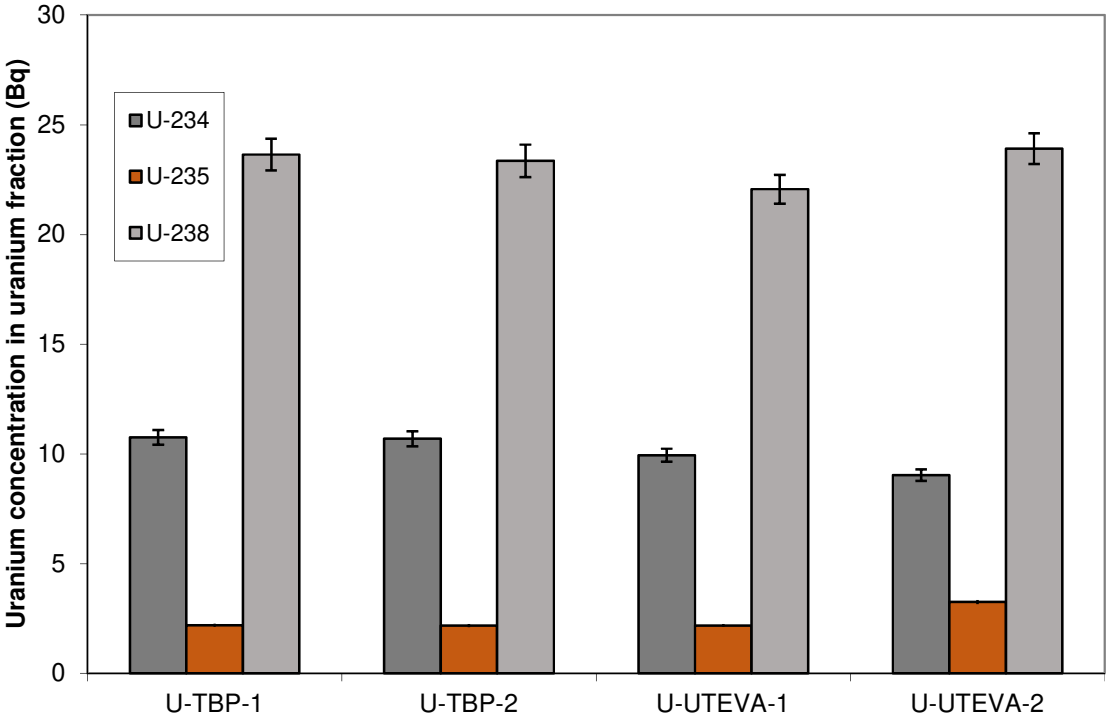

Fig. 2. Activity concentration (Bq) and isotopic ratios of the uranium isotopes using the radiochemical method with TBP (U-TBP-1 and U-TBP-2) and the radiochemical method with UTEVA (U-UTEVA-1 and U-UTEVA-2).

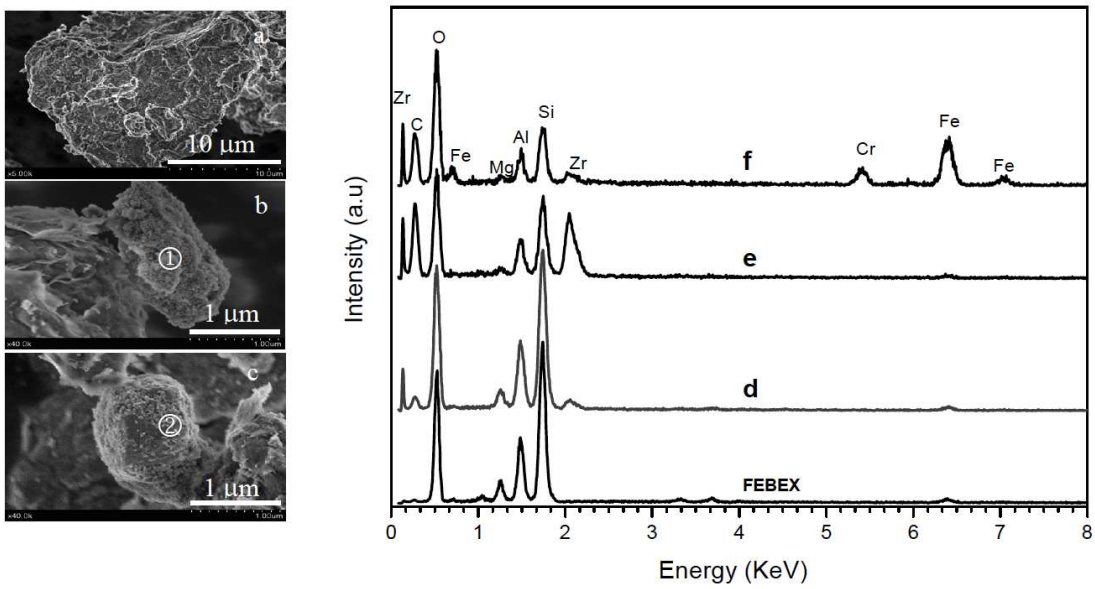

442

443 **Fig. 3**. SEM micrographs of the reacted FEBEX with a solution of ZrO^{2+}: (a) a general
444 view; (b) bright particles agglomerates mainly made up of zirconium oxide ion; and (c)
445 iron particles coming from container degradation. EDX spectra of: (d) lamellar particles;
446 (e) zirconium agglomerates; (f) iron particles; and a FEBEX spectrum as reference.

447

448

449

450

451

452

453

454

455

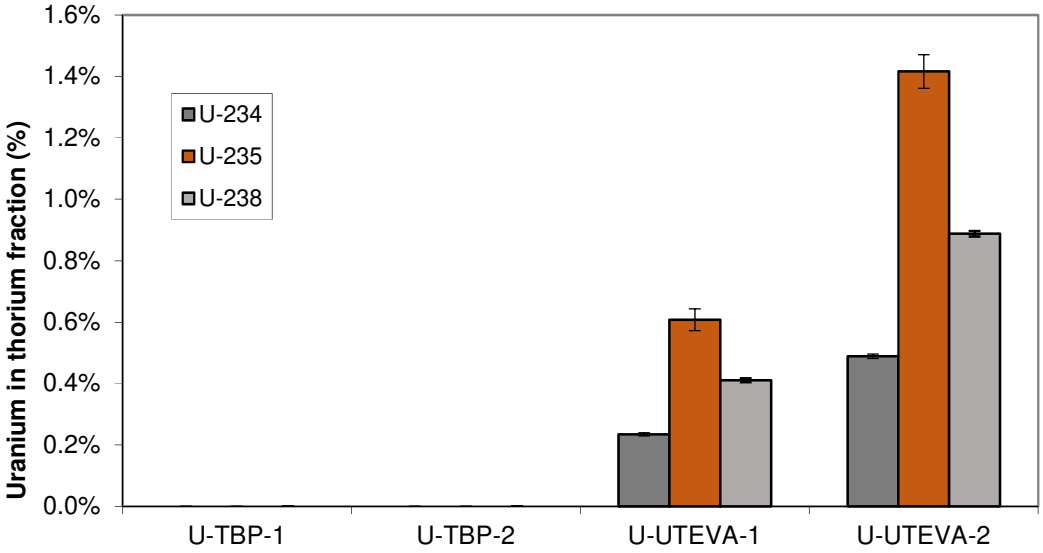

Fig. 4. Percentage of uranium measured in thorium fraction in uranyl aliquots measured by TBP (U-TBP-1 and U-TBP-2) and UTEVA (U-UTEVA-1 and U-UTEVA-2).

Figure captions

Fig. 1a. UTEVA chromatographic extraction method.

Fig. 1b. TBP liquid-liquid solvent extraction method.

Fig. 2. Activity concentration (Bq) and isotopic ratios of the uranium isotopes using the radiochemical method with TBP (U-TBP-1 and U-TBP-2) and the radiochemical method with UTEVA (U-UTEVA-1 and U-UTEVA-2).

Fig. 3. SEM micrographs of the reacted FEBEX with a solution of ZrO^{2+}: (a) a general view; (b) bright particles agglomerates mainly made up of zirconium oxide ion; and (c) iron particles coming from container degradation. EDX spectra of: (d) lamellar particles; (e) zirconium agglomerates; (f) iron particles; and a FEBEX spectrum as reference.

Fig. 4. Percentage of uranium measured in thorium fraction in uranyl aliquots measured by TBP (U-TBP-1 and U-TBP-2) and UTEVA (U-UTEVA-1 and U-UTEVA-2).

491

492

493 ## References

494 Alba, M.D., Castro, M.A., Chaín, P., Hurtado, S., Orta, M.M., Pazos, M.C., Villa, M.,
495 2011. Interaction of Eu-isotopes with saponite as a component of the engineered
496 barrier. Appl. Clay Sci. 52, 253–257. doi:10.1016/j.clay.2011.02.027
497 Alba, M.D., Chaín, P., 2007. Persistence of lutetium disilicate. Appl. Geochemistry 22,
498 192–201. doi:10.1016/j.apgeochem.2006.09.012
499 Alba, M.D., Chain, P., Orta, M.M., 2009. Chemical reactivity of argillaceous material in
500 engineered barrier. Rare earth disilicate formation under subcritical conditions.
501 Appl. Clay Sci. 43, 369–375. doi:10.1016/j.clay.2008.11.004
502 Ansari, S.A., Kumari, N., Raut, D.R., Kandwal, P., Mohapatra, P.K., 2016. Comparative
503 dispersion-free solvent extraction of Uranium(VI) and Thorium(IV) by TBP and
504 dialkyl amides using a hollow fiber contactor. Sep. Purif. Technol. 159, 161–168.
505 doi:10.1016/j.seppur.2016.01.004
506 Badr, I.H.A., Zidan, W.I., Akl, Z.F., 2014. Cyanex based uranyl sensitive polymeric
507 membrane electrodes. Talanta 118, 147–155. doi:10.1016/j.talanta.2013.10.011
508 Brennecka, G.A., Borg, L.E., Hutcheon, I.D., Sharp, M.A., Anbar, A.D., 2010. Natural
509 variations in uranium isotope ratios of uranium ore concentrates: Understanding the
510 238U/235U fractionation mechanism. Earth Planet. Sci. Lett. 291, 228–233.
511 doi:10.1016/j.epsl.2010.01.023
512 Dey, P.K., Bansal, N.K., 2006. Spent fuel reprocessing: A vital link in Indian nuclear
513 power program. Nucl. Eng. Des. 236, 723–729.
514 doi:10.1016/j.nucengdes.2005.09.029
515 Enresa, 2000. FEBEX Project. Full scale engineered barriers experiment for a deep
516 geological repository for high level radioactive waste in crystalline host rock. Final
517 Report. ENRESA Publicaciones técnicas 374.
518 Horwitz, E.P., Dietz, M.L., Chiarizia, R., Diamond, H., Essling, A.M., Graczyk, D.,
519 1992. Separation and preconcentration of uranium from acidic media by extraction
520 chromatography. Anal. Chim. Acta 266, 25–37. doi:10.1016/0003-2670(92)85276-C
521 Hurtado, S., Villa, M., 2010. An intercomparison of Monte Carlo codes used for in-situ
522 gamma-ray spectrometry. Radiat. Meas. 45, 923–927.
523 doi:10.1016/j.radmeas.2010.06.001
524 Iturbe, J.L., 1992. Identification of 236U in commercially available uranium compounds
525 by alpha particle spectrometry. Int. J. Radiat. Appl. Instrumentation. Part 43, 817–
526 818. doi:10.1016/0883-2889(92)90249-E
527 Kaufhold, S., Hassel, A.W., Sanders, D., Dohrmann, R., 2015. Corrosion of high-level
528 radioactive waste iron-canisters in contact with bentonite. J. Hazard. Mater. 285,
529 464–473. doi:10.1016/j.jhazmat.2014.10.056
530 Kumar, S., Kumar, B., Sinha, P.K., Sampath, M., Sivakumar, D., Mudali, U.K., 2017.

531 Extraction of uranium from simulated highly active feed in a micromixer-settler
532 with 30% TBP and 36% TiAP solvents. J. Radioanal. Nucl. Chem. 311, 2111–2116.
533 doi:10.1007/s10967-016-5134-5
534 Le Moigne, F.A.C., Villa-Alfageme, M., Sanders, R.J., Marsay, C., Henson, S., García-
535 Tenorio, R., 2013. Export of organic carbon and biominerals derived from 234Th
536 and 210Po at the Porcupine Abyssal Plain. Deep. Res. Part I Oceanogr. Res. Pap. 72,
537 88–101. doi:10.1016/j.dsr.2012.10.010
538 Martínez-Aguirre, A., García-León, M., Ivanovich, M., 1994. The Distribution of U, Th
539 and 226Ra derived from the phosphate fertilizer industries on an estuarine system in
540 Southwes Spain. J. Environ. Radioact. 22, 155–177. doi:10.1016/0265-
541 931X(94)90020-5
542 Mas, J.L., Villa, M., Hurtado, S., García-Tenorio, R., 2012. Determination of trace
543 element concentrations and stable lead, uranium and thorium isotope ratios by
544 quadrupole-ICP-MS in NORM and NORM-polluted sample leachates. J. Hazard.
545 Mater. 205, 198–207. doi:10.1016/j.jhazmat.2011.12.058
546 Mrabet, S. El, Castro, M.A., Hurtado, S., Orta, M.M., Pazos, M.C., Villa-Alfageme, M.,
547 Alba, M.D., 2014. Competitive effect of the metallic canister and clay barrier on the
548 sorption of Eu3+ under subcritical conditions. Appl. Geochemistry 40, 25–31.
549 doi:10.1016/j.apgeochem.2013.10.014
550 Oliveira, J.M., Carvalho, F.P., 2006. Sequential extraction procedure for determination of
551 uranium, thorium, radium, lead and polonium radionuclides by alpha spectrometry
552 in environmental samples. Czechoslov. J. Phys. 56. doi:10.1007/s10582-006-0548-x
553 Pradeep, A., Biswas, S., 2017. Purification of uranium from zirconium-rich crude sodium
554 di-uranate using counter-current solvent extraction. J. Radioanal. Nucl. Chem. 313,
555 93–99. doi:10.1007/s10967-017-5291-1
556 Skinner, M., Knight, D., 2016. The behaviour of selected fission products and actinides
557 on UTEVA® resin. J. Radioanal. Nucl. Chem. 307, 2549–2555.
558 doi:10.1007/s10967-016-4706-8
559 Villa-Alfageme, M., Hurtado, S., Castro, M.A., El Mrabet, S., Orta, M.M., Pazos, M.C.,
560 Alba, M.D., 2014. Quantification and comparison of the reaction properties of
561 FEBEX and MX-80 clays with saponite: Europium immobilisers under subcritical
562 conditions. Appl. Clay Sci. 101, 10–15. doi:10.1016/j.clay.2014.08.012
563 Villa-Alfageme, M., Hurtado, S., El Mrabet, S., Pazos, M.C., Castro, M.A., Alba, M.D.,
564 2015. Uranium immobilization by FEBEX bentonite and steel barriers in
565 hydrothermal conditions. Chem. Eng. J. 269, 279–287.
566 doi:10.1016/j.cej.2015.01.134
567 Villa, M., Manjón, G., Hurtado, S., García-Tenorio, R., 2011. Uranium pollution in an
568 estuary affected by pyrite acid mine drainage and releases of naturally occurring
569 radioactive materials. Mar. Pollut. Bull. 62, 1521–1529.
570 doi:10.1016/j.marpolbul.2011.04.003
571